Combining DT and q-space MRI: a new model of white matter in the brain

Y. Assaf[1], P. J. Basser[2]

[1]Tel Aviv Sourasky Medical Center, Tel Aviv, Israel, [2]National Institute of Child Health & Human Development (NICHD), National Institutes of Health, Bethesda, MD, United States

Synopsis

The signal decay in diffusion experiments is affected by many factors, including tissue microstructure and compartmentalization. When performing diffusion experiments at high b (or q) values, non-monoexponential signal decay is observed, especially in white matter rich areas. Here we propose a mathematical model that accounts for different modes of anisotropic diffusion (restricted and hindered) and the relative orientations of the nerve fiber axis and the diffusion gradient vectors. The model was used to fit high b value experimental diffusion data from human brain, and distinguishes between diffusion in restricted and hindered compartments.

Introduction

Diffusion tensor imaging (DTI) provides information about tissue microstructure via differences in the rate of decay of signal intensity along different directions [1]. DTI assumes a 3-D Gaussian displacement distribution [1]. While it is appropriate to use this model to describe anisotropic, hindered diffusion at low b (or q) values, it is not meaningfully applied when a deviation from Gaussian behavior is observed, especially at high b values in white matter rich areas [2]. The most likely cause of this deviation is restricted anisotropic water diffusion in the intra-axonal compartment [2]. If the slow diffusing component originates from restricted diffusion, fitting the signal decay to a bi- or multi-exponential function is inappropriate. In this work we propose a model that accounts for both restricted anisotropic diffusion within the axons and hindered anisotropic diffusion in extra-axonal compartments.

Theoretical Background

The model divides the signal attenuation in white matter into two terms: Hindered diffusion in the extra-axonal spaces and restricted diffusion in the intra-axonal space. The net signal attenuation in white matter, $E(\mathbf{q},\mathbf{\Delta})$, is described by Eq. (1) where f is the T2-weighted-population fraction of the hindered component, Δ is the diffusion time, and $\mathbf{q} = \gamma\delta\mathbf{g}/2\pi$ (γ – gyromagnetic ratio, δ – diffusion pulse duration, and $\mathbf{g}$ – diffusion gradient pulse vector). $E_r(\mathbf{q},\mathbf{\Delta})$ and $E_h(\mathbf{q},\mathbf{\Delta})$ represent the MR signal from the restricted and hindered compartments, respectively. Due to restriction, the slow exchange limit is assumed in Eq. (1).

$$E(\mathbf{q},\Delta) = f \cdot E_h(\mathbf{q},\Delta) + (1-f) \cdot E_r(\mathbf{q},\Delta) \qquad (1)$$

$$E(\mathbf{q},\Delta) = \int \bar{P}_s(\mathbf{R},\Delta)\exp(i2\pi\mathbf{q}\cdot\mathbf{R})d\mathbf{R} \qquad (2)$$

$$E_r(\mathbf{q},\Delta) = E_{r\perp}(\mathbf{q}_\perp)\, E_{r//}(\mathbf{q}_{//}) \qquad (3)$$

$$E_h(\mathbf{q},\Delta) = \exp[-4\pi^2 \mathbf{q}^T \boldsymbol{D}\mathbf{q}\Delta] \qquad (4)$$

$$E_h(\mathbf{q},\Delta) = \exp[-4\pi^2 (|\mathbf{q}_\perp|^2 \lambda_\perp + |\mathbf{q}_{//}|^2 \lambda_{//})\Delta] \qquad (5)$$

The *restricted* compartment: We assume that this compartment is composed mainly of water diffusing in the intra-axonal spaces with a signal decay is given in Eq. (2), where $\bar{P}_s(\mathbf{R},\Delta)$ is the displacement distribution. We then invoke the requirement that displacements parallel and perpendicular to the axis of the cylindrical nerve fiber are statistically independent. We also separate $\mathbf{q}$ into components parallel and perpendicular to the axon's axis, (i.e., $\mathbf{q} = \mathbf{q}_{//} + \mathbf{q}_\perp$). Then, Eq. (2) simplifies to Eq. (3). Thus, the net MR signal from the restricted compartment can be expressed as the product MR signals caused by displacements parallel and perpendicular to the axon's main axis, $E_{r//}(\mathbf{q}_{//})$ and $E_{r\perp}(\mathbf{q}_\perp)$, respectively. $E_{r\perp}(\mathbf{q}_\perp)$ can be modeled using Callaghan's formula for diffusion in impermeable cylinders [4]. $E_{r//}(\mathbf{q}_{//})$ can be modeled using the Stejskal-Tanner equation for free 1-D Gaussian diffusion. Eq. (3) is a 3-D model of anisotropic restricted diffusion.

The *hindered* compartment: We assume that this compartment is composed mainly of water diffusion in the extracellular spaces and exhibits free Gaussian diffusion. In general, this diffusion process can be anisotropic, and thus is characterized by an effective diffusion tensor, $\boldsymbol{D}$, as given by Eq. (4) [3]. This expression simplifies to Eq. (5) if we further assume that the anisotropic hindered diffusion process is caused by increased tortuosity caused by the restricted nerve fibers (and extracellular structures aligned with them). In this case, the principal axis of $\boldsymbol{D}$ coincide with the main axes of the restricted compartment.

In general there are 6 free parameters in this model: f - the T2-weighted-population fraction of the hindered component, θ and ϕ - the angles in spherical coordinates specifying the orientations of the unknown white matter fibers, $D_{//}$ - the diffusion coefficient of water inside the axon parallel to the fiber axis, $\lambda_{//}$ - the principal diffusivity in the extra-axonal spaces along the fibers, and $\lambda_\perp$ - the principal diffusivity in the extra-axonal spaces perpendicular to the fibers.

Results

Figure 1 shows how the diffusion signal decays in a pixel from the corpus callosum of a healthy volunteer. Superimposed on the data points is the fit using the model above. The model fits the signal decay along six directions simultaneously using the following parameters: $D_{//} = 1.1\text{x}10^{-5}$ cm^2/s, $\lambda_{//} = 1.1\text{x}10^{-5}$ cm^2/s, $\lambda_\perp = 0.49\text{x}10^{-5}$ cm^2/s, f = 0.60, $\theta = 0.1^0$ and $\phi = 7.8^0$.

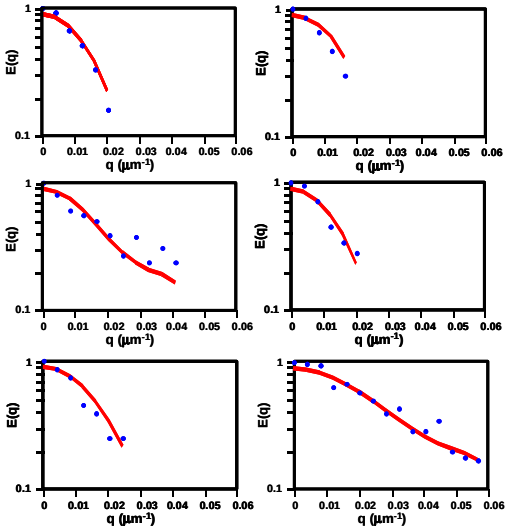

Figure 1: Experimental signal decay data (blue circles) taken from a pixel in the corpus callosum of a healthy volunteer using six gradient directions: xy, xz, yz, -xy, -xz, y-z. Red lines represent the model fit to the data. Experiments were performed on a 1.5T GE scanner with a maximal b value of 14,000 s/mm^2 (Δ/δ=71/65ms, TR/TE=2000/167ms).

Discussion

The model presented here fits the net diffusion signal decay at both low and high b (or q) values. It accounts for the effects of restricted and hindered diffusion as well as diffusion anisotropy. The contributions from hindered (Gaussian) anisotropic diffusion effects predominate at low q values, whereas the contributions from restricted anisotropic diffusion effects predominate at high q values. Figure 1 shows significant contributions due to restricted diffusion in the yz and y-z directions, which is consistent with the alignment of the nerve fibers (along the x direction) in the corpus callosum. This finding implies that this model furnishes additional information with which to determine fiber direction(s) in each pixel. Indeed, the θ and ϕ angles, as determined by the fit, show that the nerve fibers lie along the x direction.

Callaghan's formula for diffusion within impermeable cylinders requires specifying the diameter distribution. In this model we assumed a given histological axon diameter distribution. However, in cases when the distribution is unknown, it may be possible to estimate features of this distribution as free parameters in the fitting procedure. The number of free parameters in the model is still equal to the number of underdetermined diffusion tensor elements estimated in a DT-MRI experiment, six making this model clinically feasible to apply.

Conclusion:

This new model combines and synthesizes the 3-D tensor description of anisotropic hindered diffusion in the extra-axonal compartment and a 3-D model of restricted anisotropic diffusion in the intra-axonal compartment using a small number of physically reasonable assumptions. The ability to discriminate between diffusion within intra- and extra-axonal compartments might better explain the origin of diffusion anisotropy observed in DWIs, as well as changes in diffusion MR data observed in development, degeneration, disease and aging.

References

[1] Basser PJ. *NMR Biomed* **8**, 333-344 (1995). [2] Assaf Y, Cohen Y. *Magn. Reson. Med.* **43**, 191-199 (2000). [3] Basser PJ. *Magn. Reson. Med.* **47**, 392-397 (2000). [4] Callaghan PT. *J Magn. Reson. A* **113**, 53-59 (1995).